Electrothermally Actuated Silicon Carbide Tunable MEMS Resonators

Electro-thermally Actuated Silicon Carbide Tunable MEMS Resonators

Enrico Mastropaolo, Graham S. Wood, *Member, IEEE*, Isaac Gual, Philippa Parmiter, and Rebecca Cheung, *Senior Member, IEEE*

***Abstract*—This paper presents the fabrication and characterisation of SiC flexural-mode structures able to operate as electro-thermo-mechanical tunable resonators. Single and double clamped beams, as well as circular structures, have been fabricated with aluminium (Al) and platinum (Pt) top electrodes. Electro-thermal excitation has been used for device actuation, resonant frequency tuning and mixing. Circular structures (i.e. disks) have been shown to possess higher resonant frequencies and Q-factors (up to ~23,000) compared to beams having similar dimensions. Tuning of the resonant frequency has been performed by varying the DC and AC component of the actuating voltage on SiC beams with u-shaped and slab Pt electrodes. When increasing the DC bias, frequency shift rates of about -11,000 ppm/V and -1,100 ppm/V are measured for the u-shaped and slab electrodes, respectively. When increasing the amplitude of the AC input, shift rates of about -1,800 ppm/V and - 800 ppm/V are measured. In addition, measurements have shown that the frequency shift rate increases with the ambient temperature. Electro-thermal mixing has been performed by applying two actuating voltages with the sum or difference of their frequencies matching the fundamental resonance of the SiC structure. Tuning of the electro-thermally mixed output singal has been demonstrated on a disk resonator.**

***Index Terms* — Electro-thermal transduction, actuation, tuning, mixing, resonators, silicon carbide.**

I. Introduction

DEVICES such as gyroscopes, pressure sensors, accelerometers, micro-switches and micro-mirrors have been developed using micro-electromechanical systems (MEMS) for use in a variety of applications including telecommunications, optics, biomedicine, automotive industry [1] and challenging applications such as quantum mechanical devices [2] and energy harvesting [3]. In systems requiring timing and frequency control functions, MEMS are considered as possible solutions to overcome size reduction and power consumption issues [4], [5], [6], [7]. In particular, in the last decade, much attention has been focused on the use of MEMS resonators for applications such as real time clocks [6], reference oscillators [8], and filters/mixers in the front-end of wireless transceivers [9] [10].

Electro-static excitation is a widely used technique for MEMS actuation allowing more flexible structures' geometries [7]. Despite a slower response and higher power consumption compared to electro-static techniques, electro-thermal excitation is considered a good solution to overcome major drawbacks such as critical fabrication steps, impedance matching and relatively high actuation voltages that are typical of electro-static transduction [11]. Si resonators actuated electro-thermally have shown good performance as MEMS filters [12]. Recently, dome resonators have been actuated with the input signal being the superimposition of two signals through a linear power combiner [12].

For reliable operation in harsh environments, silicon carbide (SiC) is expected to be a superior material due to its robustness, chemical inertness and radiation resistance [10][11]. In addition, SiC devices can resonate at higher frequencies compared to silicon (Si) devices with similar dimensions due to SiC's relatively large ratio of Young's modulus E to mass density ρ [14] [15].

The capability of tuning the resonant frequency of MEMS resonators is desirable for many applications. In particular, tuning can be used to compensate for a drift in the resonator's frequency that may occur due to changes in ambient temperature, pressure or atmosphere composition [16]. Also, tuning can be used when the fabrication process affects the dimensions of the structure thus influencing the predicted frequency. In addition, signal processing applications such as frequency-hopping can be addressed by tuning the device's resonance [17].

Manuscript received May 4, 2011.

This work was supported in part by Scottish Enterprise.

E. Mastropaolo, and R. Cheung are with the Scottish Microelectronics Centre, Institute for Integrated Micro and Nano Systems, School of Engineering, The University of Edinburgh, EH9 3JF, UK (phone: +44-131-650-7471; fax: +44-131-650-7475; e-mail: e.mastropaolo@ed.ac.uk; r.cheung@ed.ac.uk).

G. S. Wood was with the Scottish Microelectronics Centre, Institute for Integrated Micro and Nano Systems, School of Engineering, The University of Edinburgh, UK. He is now with the Nano Research Group, School of Electronics and Computer Science, University of Southampton, SO17 1BJ, UK (e-mail: gsw1g11@ecs.soton.ac.uk).

I. Gual was with the Scottish Microelectronics Centre, Institute for Integrated Micro and Nano Systems, School of Engineering, The University of Edinburgh, UK. He is now with Intesis Software SL, Barcelona, Spain (e-mail: igual@intesis.com).

P. Parmiter was with the Scottish Microelectronics Centre, Institute for Integrated Micro and Nano Systems, School of Engineering, The University of Edinburgh, UK. She is now with the Scottish Institute of Sustainable Technology, James Nasmyth Building, Edinburgh, EH14 4AS, UK (e.mail: philippa.parmiter@sistech.co.uk).

In this paper, we demonstrate the operation of bimaterial metal/SiC structures as micro-electro-thermo-mechanical resonators for real time clock applications and frequency-setting devices. The devices have been simulated, fabricated and tested. In particular, SiC vertical resonators designed as single clamped beams (i.e. cantilevers), clamped-clamped beams (i.e. bridges) and circular structures (i.e. disks with a small hole/aperture in the middle) with top aluminium (Al) and platinum (Pt) electrodes have been studied. Also, lead zirconium titanate (PZT) films have been fabricated on top of the structures in order to demonstrate the possibility of integrating piezo-electric sensing ports [18]. However, the piezo-electric ports have not been used for the work presented here.

The role of the design and structure dimensions on the resonant frequency has been investigated by actuating the devices mechanically. Electro-thermal actuation has been performed by applying an input AC voltage superimposed to a DC bias to the top electrodes. Tuning of the resonant frequency has been achieved by varying the DC bias and AC amplitudes of the input actuating signal. Finite element simulations (FEM) have been used to analyse the mechanism of electro-thermal tuning. In addition, the tuning capability of two different electrode configurations (u-shaped and slab) has been investigated at different ambient temperatures. Electro-thermal mixing of two input signals has been carried out on the fabricated Al/SiC cantilevers and disks; the tuning of the mixed frequency has been demonstrated by varying the DC bias of one of the actuating voltages.

II. Theory

A. Resonant frequency

The impact of different structure dimensions on the resonant frequency is an important factor when MEMS are to be employed for telecommunication and timing applications. The fundamental resonant frequency of a structure is determined by both its dimensions and the mechanical properties of the material. The structure's dimensions are defined during the design and fabrication processes. The formulae for the fundamental mechanical resonant frequencies of cantilevers f_C, bridges f_B and disks f_D are as follows:

$$f_C = 0.162\sqrt{\frac{E}{\rho}}\frac{t}{L^2} \quad , \qquad (1)$$

$$f_B = 1.03\sqrt{\frac{E}{\rho}}\frac{t}{L^2} \quad , \qquad (2)$$

$$f_D = 1.65\sqrt{\frac{E}{\rho}}\frac{t}{D^2} \quad , \qquad (3)$$

where E and ρ are the Young's modulus and mass density of the structure's material, respectively, t is the thickness of the structure, L is the length of the beam and D is the diameter of the disk [19], [20]. From (1), (2) and (3), for comparable dimensions, a disk exhibits a fundamental mechanical resonant frequency ~10 times higher than a cantilever and ~6.4 times higher than a bridge.

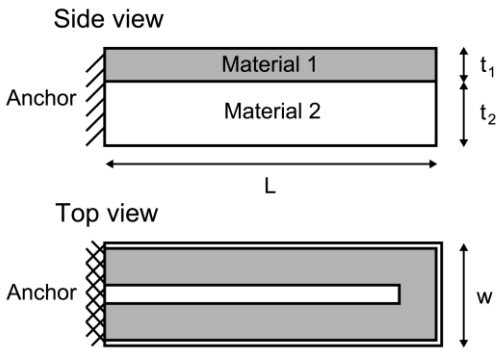

Fig. 1. Schematic configuration of a bimaterial cantilever.

B. Electro-thermal actuation

A device is actuated electro-thermally by inducing a thermal expansion of the structure. The advantages of electro-thermal actuation include simplified fabrication and relatively low operating voltages [21].

In general, bimaterial structures are employed so that one material is used as actuation electrode and the other one as the structure to be actuated. When a voltage is applied across the actuation electrode, Joule heat is generated as a result of the electric current that is dissipated through the electrode resistance. Under these conditions, a temperature gradient ΔT is induced leading to a mechanical strain experienced within the structure. The difference between the two materials' thermal expansion coefficients (TEC) $\Delta\alpha$ serves to increase the mechanical strain. For example, Fig. 1 shows the schematic of a bimaterial cantilever. In this case, the blocked moment M_b can be derived by using Timoshenko bimetallic strip theory and written as [22]:

$$M_b = \frac{b}{2}\Delta\alpha \cdot \Delta T \quad , \qquad (4)$$

where b is a constant dependent on the beam geometry and the materials' Young's modulus:

$$b = \frac{E_1 t_1 \cdot E_2 t_2 \cdot (t_1 + t_2)w}{(E_1 t_1 + E_2 t_2)} \quad . \qquad (5)$$

If the temperature change is induced by an applied voltage and the heat is transferred only by conduction, ΔT can be written as a function of power dissipated per unit volume P_V and equivalent thermal conductivity K_{eq} [22]:

$$\Delta T \approx \frac{P_V L^2}{3K_{eq}} \quad , \qquad (6)$$

with

$$K_{eq} = \frac{K_1 t_1 + K_2 t_2}{t_1 + t_2} \quad . \qquad (7)$$

The blocked moment M_b as a function of the power per unit volume P_V can be obtained by combining (4) and (6):

$$M_b \approx \frac{bL^2}{6} \cdot \frac{\Delta\alpha}{K_{eq}} \cdot P_V \quad . \qquad (8)$$

From (8), the actuating force is proportional to the dissipated power and therefore to the square of the applied voltage. The device can be driven into motion by applying an alternating voltage across the input electrode causing mechanical vibration at the same frequency as the voltage [21] [22].

As an example, Fig. 2a shows a schematic of an input voltage connected to an electrode placed on top of a cantilever. If the input voltage V_1 equals $V_{ac1} sin\ \omega_{ac1}t + V_{dc1}$, the power dissipated in the electrode with resistance R is given by:

$$P = \frac{V_1^2}{R} = \frac{(V_{ac1} \sin \omega_{ac1} t + V_{dc1})^2}{R} \quad . \qquad (9)$$

The AC component of the power is obtained by expanding (4) and neglecting the DC terms:

$$P_{ac} = \frac{2V_{dc1}V_{ac1}}{R} \sin \omega_{ac1} t - \frac{V_{ac1}^2}{2R} \cos 2\omega_{ac1} t \quad . \qquad (10)$$

If the actuation signal V_1 contains both an AC and a DC component, the device is driven into resonance when the input frequency $f_{ac1} = \omega_{ac1}/2\pi$ matches the structure's natural frequency f_0. If V_1 is a purely AC signal with no DC bias then the structure is driven into resonance if $f_{ac1} = f_0/2$ [21].

C. Electro-thermal tuning – thermal stress

The resonant frequency of a device can be shifted by

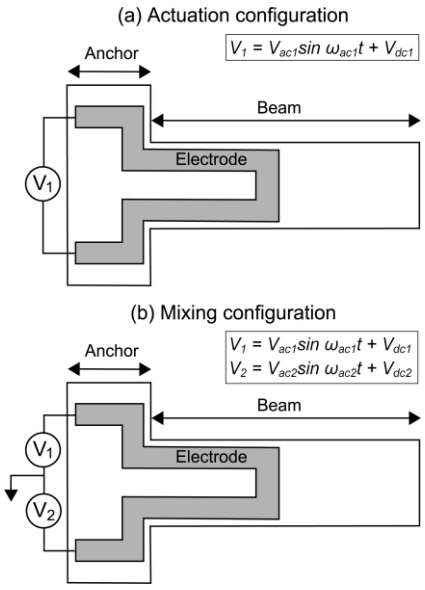

Fig. 2. Schematic configuration of a cantilever with electro-thermal actuation (a) and mixing (b).

inducing an expansion or contraction of the structure electro-thermally. The change in length δ_L of a material experiencing a uniform change in temperature ΔT is proportional to the TEC α and can be written as:

$$\delta_L = \alpha L \Delta T \quad , \qquad (11)$$

where L is the initial length of the material in the given direction. If the expansion of the material is impeded by the interaction to another material, a thermal stress σ_T is induced:

$$\sigma_T = \frac{-\delta_L E}{L} \quad . \qquad (12)$$

If the material is prevented from expanding the stress experienced can be obtained by combining equations (10) and (11) [23]:

$$\sigma_T = -\alpha E \Delta T \quad . \qquad (13)$$

In the experiments performed, a thermal stress is induced in the structures as a consequence of the DC bias of the electro-thermal actuation. It is believed that the thermal stress is governed mainly by two mechanisms: the expansion of the beam and the expansion of the Si substrate at the anchors. The mechanical resonant frequency of a structure is influenced by the stress experienced. For instance, in the case of a bridge structure, an increasing compressive stress results in an decrease of the resonant frequency while an increasing tensile stress results in an increase of the frequency [17].

D. Electro-thermal mixing

In order to perform a mixing function, two input voltages are applied to the input electrode. As an example, Fig. 2b shows the schematic configuration of two input voltages applied to an electrode placed on top of a cantilever. In this case, the power dissipated is given by:

$$P = \frac{(V_{ac1} \sin \omega_{ac1} t - V_{ac2} \sin \omega_{ac2} t + V_{dc1} - V_{dc2})^2}{R} \quad . \qquad (14)$$

The AC component of the power is obtained by expanding (9) and neglecting the components $cos(2\omega_{ac1}t)$ and $cos(2\omega_{ac2}t)$:

$$P_{ac} \propto \frac{V_{ac1}V_{ac2}\left[\cos(\omega_{ac1} + \omega_{ac2})t - \cos(\omega_{ac1} - \omega_{ac2})t\right]}{R} \quad . \qquad (15)$$

Therefore, the mechanical force exerted on the resonator is proportional to both the sum and difference of the frequency components of the applied voltage. As a result, the device will be driven into resonance if the sum or difference of the input frequencies equals the natural resonant frequency of the structure f_0 [24].

III. Experimental procedure

Cantilever, bridge and disk structures have been fabricated in order to characterise their different resonant behaviour and to achieve a wide range of resonant frequencies.

A. Fabrication

Fig. 3 shows the fabrication process flow for cantilevers, bridges and disks designed with top electrodes to be used for electro-thermal actuation. A 2 µm thick layer of single crystalline 3C-SiC has been grown on a Si substrate using a two-step carbonisation-based atmospheric pressure chemical vapour deposition process [25]. A 100 nm passivation layer of thermal oxide has been grown on top of the SiC epilayer (Fig. 3a). Then, a metal layer has been deposited (500 nm Al or 100 nm Pt) on top of the thin oxide layer (Fig. 3b). The metal and the underlying oxide have been patterned and etched using reactive ion etching (RIE) for Al and argon ion beam for etching Pt (Fig. 3c). After, an oxide layer has been deposited

(Fig. 3d), patterned and etched (Fig. 3e) to form the mask for SiC etching. The SiC is etched and the underlying Si partially released (Fig. 3f) using inductively coupled plasma (ICP) with a mixture of SF_6 and O_2 [26]. XeF_2 chemical etching has been performed in order to complete the removal of the Si underneath the structures (Fig. 3g). Finally, RIE has been used to remove any remaining masking oxide (Fig. 3h).

In addition, the process flow for the Pt/SiC bridges has been extended in order to integrate a 500 nm thick layer of piezo-electric PZT on top of the devices. The PZT layer has been

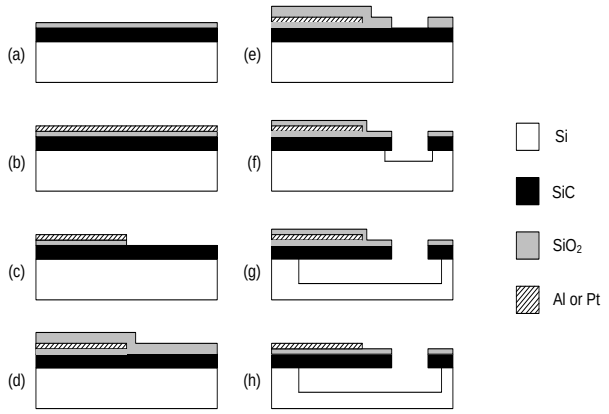

Fig. 3. Schematic of the process flow used for the fabrication of the SiC structures.

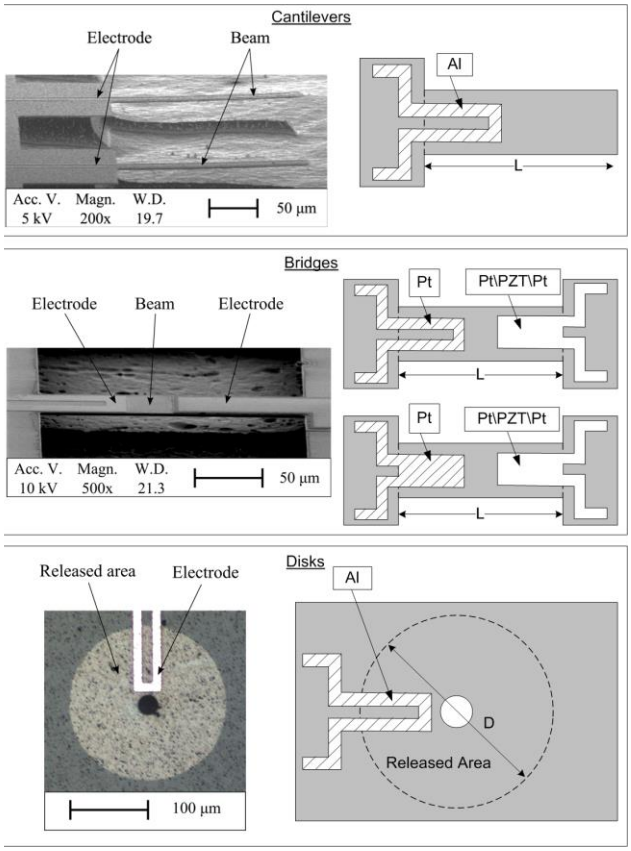

Fig. 4. Scanning electron and optical micrograph images of some of the fabricated SiC structures along with their schematics.

sandwiched between two Pt layers and the resulting Pt/PZT/Pt stack patterned to form a piezo-electric port [27]. The extended process flow allows the fabrication of Pt electrodes and Pt/PZT/Pt ports on the same device for possible use as input actuators and output sensors for the resonator, respectively [18].

Fig. 4 shows the scanning electron and optical micrographs together with the schematics of some of the fabricated structures with top metal electrodes. The devices have been fabricated with the length/diameter varying between 50 µm and 300 µm. Pt electrodes with u-shaped and slab architectures have been fabricated on some SiC bridges in order to investigate the influence of electrode design on electro-thermal tuning. For this study, Pt has been chosen because of its compatibility with PZT processing and excellent reliability characteristics compared to Al when used as electro-thermal actuating electrode for SiC resonators operating at ambient temperatures from 10 ºC to 100 ºC [28].

B. Measurements

The resonant frequency of the fabricated devices has been investigated in vacuum (~0.001 mbar) with a Polytec OFV-3000 laser vibrometer. Fig. 5 shows the schematic of the measurement set-up. Initial studies on the fundamental resonant frequency have been carried out by mounting the devices on a piezo-electric disk actuated with an AC voltage. With this set-up, the mechanical vibrations induced to the piezo-electric disk are transferred to the tested devices so that the resonance of the structures could be investigated.

For performing electro-thermal actuation, an AC voltage with amplitude V_{ac1} has been superimposed to a DC bias V_{dc1} and applied to the devices' metal electrodes (see Fig. 2a). The chips with the fabricated devices have been wire bonded on a chip carrier and plugged into a PCB socket. The input signal amplitudes have been set at V_{ac1} = 4 V and V_{dc1} = 1 V for actuating beams and at V_{ac1} = 6 V and V_{dc1} = 2 V for actuating disks. Under these conditions, the resonant frequency and the vibration amplitude has been measured with the laser vibrometer. The quality factor Q has been calculated from the measured frequency response of the devices. In addition to the measurements performed in vacuum, some of the

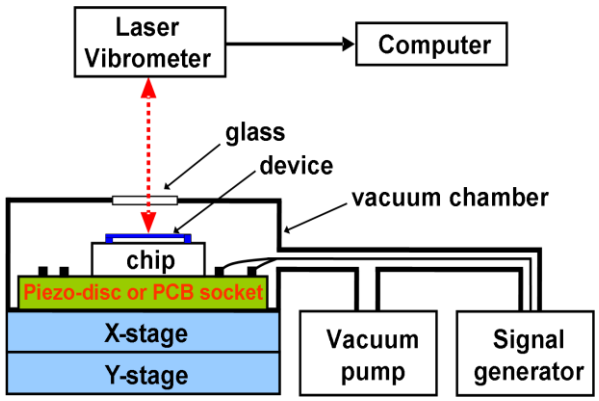

Fig. 5. Measurements set-up for mechanical or electro-thermal actuation and optical detection.

fabricated disks have been actuated electro-thermally at atmospheric pressure and their resonance investigated with a Polytec UHF vibrometer.

Electro-thermal mixing has been performed on cantilevers by applying two input voltages to the actuating electrodes (see Fig. 2b). In this case, the AC and DC amplitudes have been fixed at $V_{ac1} = V_{ac2} = 4$ V and $V_{dc1} = V_{dc2} = 1$ V, one of the input frequencies has been fixed while the other one has been varied. In addition, the possibility of tuning the resonant frequency when mixing on a disk structure has been investigated. In this case, the AC voltage amplitudes have been held at $V_{ac1} = V_{ac2} = 6$ V, the DC bias V_{dc2} at 2 V and the resonance monitored while varying V_{dc1} from 2 V to 0.5 V.

The investigations on the electro-thermal tuning of the bridges with Pt electrodes (u-shaped and slab), have been carried out in a temperature-controlled vacuum chamber (~0.001 mbar). In these experiments, the temperature has been held at 25˚C and the resonance has been monitored while the DC bias V_{dc1} has been increased from 1 V to 4 V and the AC drive voltage V_{ac1} from 2 V to 3 V. In order to investigate the influence of ambient temperature, additional electro-thermal tuning experiments have been conducted by increasing the temperature of the chamber from 10˚C to 100˚C.

C. Simulations

Finite element simulations (FEM) have been performed using *CoventorWare*. FEM analysis has been used as a complementary tool to study the changes in temperature and stress experienced by the devices when performing electro-thermal actuation and tuning. FEM simulations have been shown to be useful for investigating the temperature and stress gradients throughout the structures and their anchors. For these investigations, the structures depicted in the schematics of Fig. 4 have been simulated.

IV. Results and Discussion

A. Mechanical actuation

The fabricated SiC cantilevers, bridges and disks with different dimensions have been actuated mechanically and their fundamental resonant frequency monitored with the optical vibrometer. Fig. 6 shows the measured frequency as a function of beam length L and disk diameter D. The frequency values calculated with the analytical formulas (1), (2) and (3) have been plotted for comparison.

In agreement with the analytical formulas, for similar dimensions, disks resonate at higher frequencies compared to beam architectures and cantilevers possess the lowest frequencies. The inset of Fig. 6 shows one of the resonant peaks obtained for a disk with $D = 250$ µm (Q ~ 8,500). The frequencies measured for disk structures are higher than the analytical ones calculated with (3). It is important to notice that the analytical formula describes the behaviour of plain disks neglecting the influence of a central hole and of the

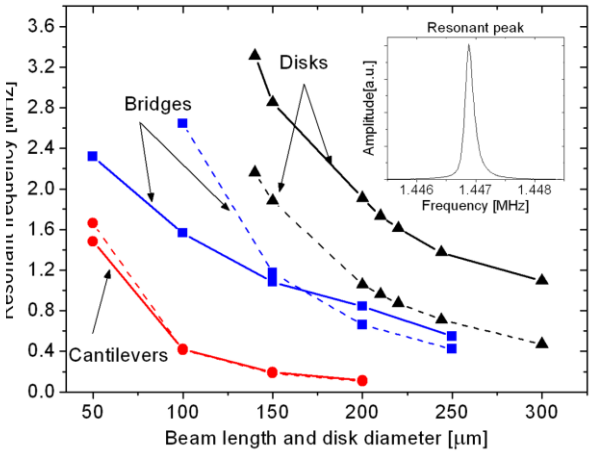

Fig. 6. Measured (solid line) and theoretical (dashed line) resonant frequency as a function of structure dimensions (inset: resonant frequency peak measured for a disk with diameter $D = 250$ µm).

internal stress on the frequency. It has been reported that the presence of a central hole results in an increase of the resonant frequency of disks [19]. In addition, it is believed that the fabricated disks possess a relatively high tensile stress due to the manufacturing process thus resulting in an increase of the resonant frequency. Also, differences between the predicted and measured frequencies have been obtained for cantilever lengths $L < 100$ µm and bridge lengths $L < 150$ µm. This effect is due mainly to the undercut at the structures' anchors that is a consequence of the sacrificial release method used for the fabrication (see Fig. 3g) [29]. The undercut for cantilevers and bridges has been measured to be ~ 5 µm and 30 µm, respectively. Under these conditions, the effective beam length is longer than the designed one thus contributing to a higher resonant frequency with a greater influence on shorter beams.

B. Electro-thermal actuation

Electro-thermal actuation has been performed on the structures fabricated with Al and Pt u-shaped and slab electrodes. Devices having similar configurations to the ones depicted in Fig. 4 have been driven into resonance by applying an actuation voltage to the top electrodes (see Fig. 2a).

Fig. 7 shows two of the resonant peaks measured when actuating electro-thermally a SiC cantilever (~ 89.5 kHz) and a disk (~ 891.5 kHz) with Al u-shaped electrodes. In vacuum, vibration amplitudes of ~ 0.5 µm and Q-factors up to ~ 23,000 have been measured with disk resonators exhibiting quality factors higher than beam resonators. Smaller amplitudes and lower Q-factors have been obtained when actuating the devices at atmospheric pressure.

As an example, Figs. 8(a) – (d) show the measurements snapshots obtained when actuating a disk resonator at atmospheric pressure. In this case, due to the relatively small dimensions and the structure design, a double u-shaped electrode configuration (Fig. 8a) has been needed in order to obtain detectable vibration amplitudes (in the range of 5 to 10 pm) for the first (b), second (c) and third (d) modes at 7.79 MHz, 27.57 MHz and 49.38 MHz, respectively.

C. *Electro-thermal tuning*

As discussed in II.C., the tuning of the resonant frequency can be performed by inducing temperature changes electro-thermally and therefore varying the thermal stress within the structure. Electro-thermal tuning is expected to be particularly feasible when used alongside electro-thermal actuation removing the need of additional tuning electrodes or post-fabrication structural adjustments.

The resonant frequency of SiC bridges with top Pt u-shaped and slab electrode architectures (Fig. 4b) has been tuned

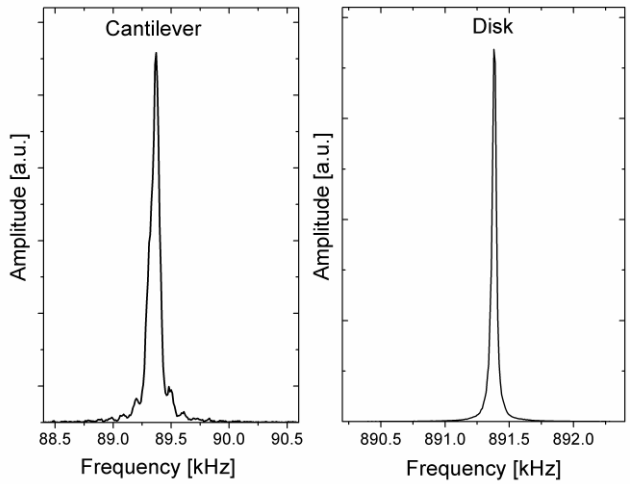

Fig. 7. Electro-thermal actuation: measured resonant peaks for a cantilever (L = 200 µm, Q ~ 2000) and disk (D = 380 µm, Q ~ 22300).

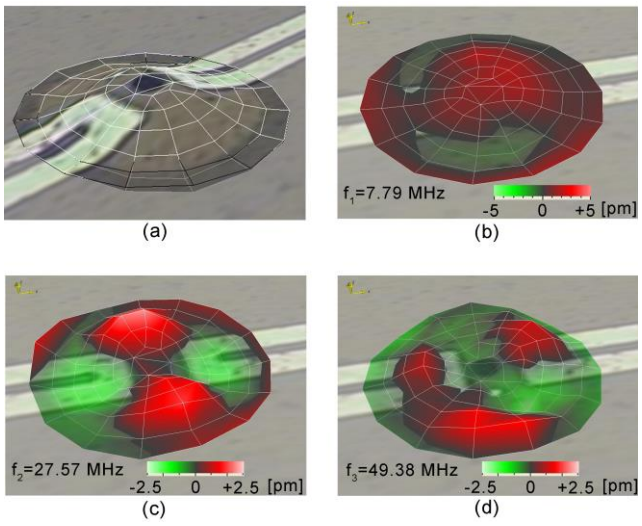

Fig. 8. Measurements snapshots of a disk actuated electro-thermally with D = 90 µm: static deflection (a), first mode (b), second mode (c), third mode (d).

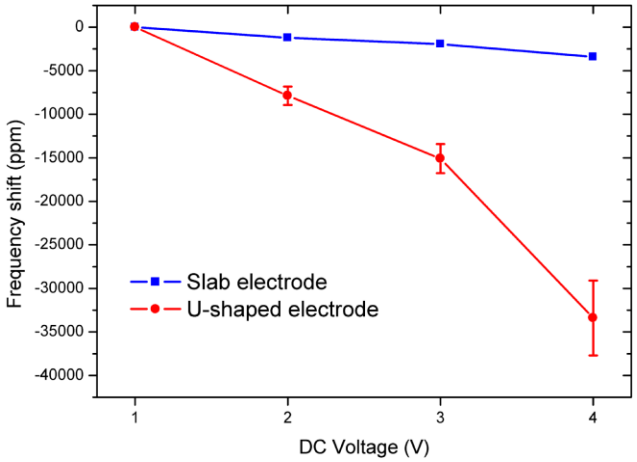

Fig. 9. DC bias variation: measured frequency shift relative to the value at V_{DC} = 1 V for u-shaped and slab electrodes. Error bars represent the maximum and minimum values from measurements of multiple devices.

electro-thermally. In particular, the resonant frequency has been shifted by varying the AC and DC components of the input actuating voltages.

1) *Variations of DC amplitude – frequency tuning*

Electro-thermal tuning has been performed by varying the DC component of the actuation signal. When the input DC bias is changed, the temperature induced within the structure changes resulting in a variation of the thermal stress and, consequently, in a shift of the resonant frequency. The effect of DC voltage variations on the resonant frequency has been characterised by fixing the AC amplitude V_{ac1} = 4 V while increasing the DC bias voltage V_{dc1} from 1 to 4 V (see Fig. 2a). Furthermore, the different response of the u-shaped and slab electrodes to DC bias variations has been investigated.

Fig. 9 shows the resonant frequency shift measured as a function of the DC voltage when induced with the u-shaped and slab electrode designs. The resonant frequency has been shown to decrease as the DC bias is increased regardless of the electrode configuration used. The increase of the DC voltage induces an increase of temperature within the structure enhancing the thermal expansion of the beam and of the substrate's material at the anchor that results in a shift of the resonant frequency. It is believed that the resonant frequency decreases because of the compressive behaviour of the induced stress [17].

From Fig. 9, the u-shaped electrode induces a larger frequency shift compared to the slab one. In particular, the measurements have shown a shift of -35,000 ppm with a rate of about -11,000 ppm/V with the u-shaped layout and a shift of -3,500 ppm with a rate of about -1,100 ppm/V with the slab electrode. The measured devices exhibit a greater frequency variation compared to previously reported results of -11 ppm/V that have been achieved actuating a lateral resonator electro-statically [30]. The greater variation indicates that DC thermal heating has a greater influence on the stress than an electrostatic force. Another study [17] reported frequency variation of -50,000 ppm/V for the electro-thermal tuning of a 2.5 µm long SiC bridge with thickness and width of ~ 30 nm.

When compared to the devices in our study, the much greater frequency shift measured in [17] is probably due to the smaller dimensions.

The influence of DC bias variations on the temperature and on the stress experienced by the devices with u-shaped and slab Pt electrodes has been investigated further with FEM analysis. As reported previously [18], a decrease in resonant frequency (Fig. 9) suggests that the beam is experiencing increasing compressive stress as a result of thermal heating.

Fig. 10 shows the simulated temperature profile along the beam when applying DC actuating voltages in the range 1 – 4 V with u-shaped (dash-dot line) and slab (solid line) electrodes. The temperature increases as the bias voltage increases because of the direct proportionality to the electrical power dissipated in the electrode and consequently to the square of the input voltage (see (10)). In agreement with previously reported simulations [31], when comparing the two electrode designs, the simulation results confirm that u-shaped electrodes induce a higher temperature at the centre of the beam (position along the beam ~ 0.5 in Fig. 10) while slab electrodes induce a higher temperature at the anchor (position along the beam < 0.1 in Fig. 10). Fig. 11 shows the simulation results for the average compressive stress on the longitudinal axis (i.e. along the length of the beam) as a function of the bias voltage. As the DC voltage is increased from 1 V to 4 V, the compressive stress has been observed to increase from 25 MPa to 180 MPa and from 50 MPa to 400 MPa for the slab and u-shaped architectures, respectively.

The simulations have confirmed that the temperature increases when the DC voltage is increased. The results show that the increase of temperature enhances the thermal expansion of the entire structure (beam and anchors) thus inducing a compressive force on the beam, lowering the resonant frequency.

The differences in the resonant frequency shift and shift rate obtained with the two different electrode configurations can be explained by observing the trend of compressive stress induced by the increase of DC bias voltage. From Fig. 11, the u-shaped architecture is shown to induce a larger variation in compressive stress (~350 MPa) compared to the slab configuration (~150 MPa) due to the fact that the heat

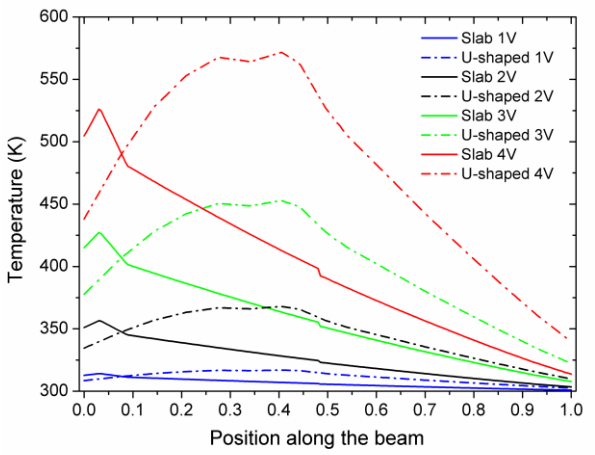

Fig. 10. Simulated temperature along the beam when applying DC voltages in the range 1 – 4 V to u-shaped (dash-dot line) and slab (solid line) electrodes.

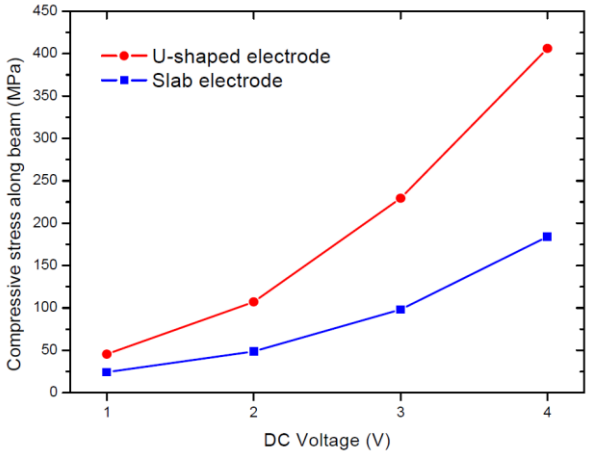

Fig. 11. Simulated total compressive stress along the beam as a function of DC bias voltage.

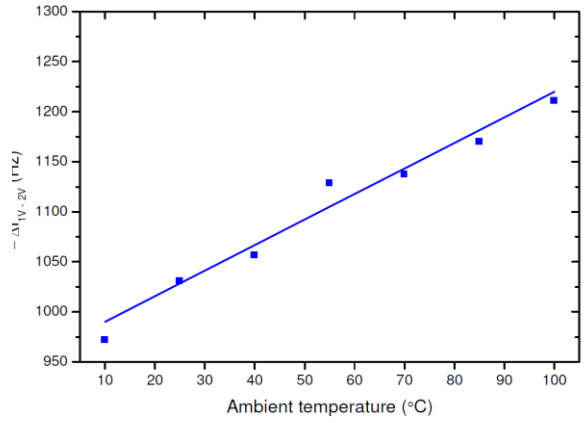

Fig. 12. Measured shift in resonant frequency measured when the DC bias is increased from 1 V to 2 V at different ambient temperatures.

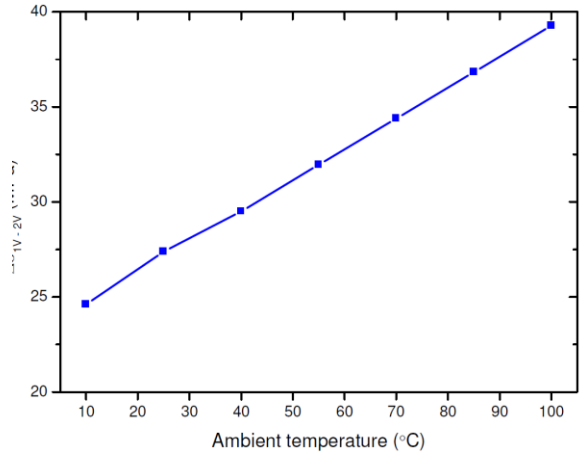

Fig.13. Simulated shift in compressive stress simulated when the DC bias is increased from 1 V to 2 V at different ambient temperatures.

generated with this configuration causes an expansion of the beam rather than an expansion at just one anchor [31]. Therefore, by inducing a larger stress variation, the u-shaped electrode induces a larger change in the resonant frequency. This result is in agreement with previously reported results showing that larger changes in stress lead to larger shifts of the resonant frequency [17].

2) Influence of ambient temperature on frequency and stress

In order to determine the influence of the ambient temperature on the devices' behaviour, the DC tuning of a bridge actuated with a slab electrode when varying the temperature T_{amb} has been investigated. Fig. 12 shows the decrease in resonant frequency when the DC bias is increased from 1 V to 2 V, $-\Delta f_{(1\text{-}2V)}$, measured over a temperature range 10 – 100 ˚C. $-\Delta f_{(1\text{-}2V)}$ has been observed to increase from 1 kHz to 1.2 kHz as T_{amb} rises from 10 to 100 ˚C.

FEM simulations have been performed in order to observe the trend of the stress experienced by the beam as a function of T_{amb}. Fig. 13 shows the simulated change in compressive stress $\Delta\sigma_{T(1\text{-}2V)}$ induced by the increase of DC bias voltage from 1 V to 2 V as function of T_{amb}. $\Delta\sigma_{T(1\text{-}2V)}$ has been shown to increase from ~ 24 MPa to ~ 38 MPa as the temperature is increased from 10 ˚C to 100 ˚C thus possibly explaining the increasing shift in resonant frequency with the temperature (Fig. 12). The increase in $\Delta\sigma_{T(1\text{-}2V)}$ as a function of temperature observed in Fig. 13 can be explained by the fact that the TEC of SiC is larger at higher temperatures thus resulting in a greater thermal expansion of the beam [32].

3) Variations of AC amplitude – frequency tuning

The influence of the amplitude of the AC actuation signal on the resonant frequency shift has been investigated. Similar to the case of DC electro-thermal tuning, AC voltage variations have been investigated on bridges having Pt u-shaped and slab electrodes and their tuning responses have been compared.

Fig. 14 shows the shift in the resonant frequency detected with the DC bias voltage fixed at 1 V and the AC amplitude increased from 2 V to 3 V. Similar to the case of DC tuning, the frequency has been shown to decrease as the AC voltage increases. The rate of frequency shift varies from -1,300 ppm/V up to -1,800 ppm/V for the u-shaped electrode and is constant ~ -800 ppm/V for the slab electrode device. The slab electrode induces a lower frequency shift compared to the u-shaped one in the voltage interval considered.

The frequency shift observed for increasing AC voltage amplitude is believed to be due to the change in the RMS voltage. The average power dissipated in the electrode due to the AC signal alone is given by $(V_{RMS})/R$, where R is the resistance of the electrode. When the AC amplitude is increased from 2 to 3 V, the RMS voltage increases from 1.41 V to 2.12 V hence leading to an increase of the power dissipated. Therefore, the frequency shifts shown in Fig. 14 can be expressed in terms of RMS voltage as ~ -2,250 ppm/V_{RMS} and as ~ -1,130 ppm/V_{RMS} for the u-shaped and slab electrodes, respectively. The shift due to the RMS voltage is around a third of the value for the DC bias voltage probably due to the alternating nature of the signal.

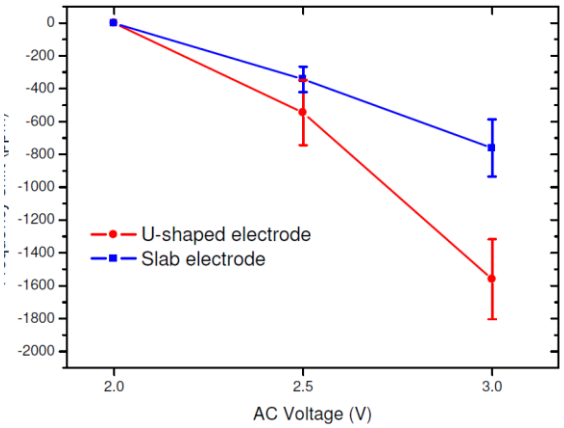

Fig. 14. AC voltage variations: measured resonant frequency shift relative to the value measured at V_{ac} = 2 V. Error bars represent the maximum and minimum values from measurements of multiple devices.

It is worth noting that the devices presented in this study exhibit a larger frequency variation as a function of AC drive voltage (-800 ppm/V) compared to reported results for a lateral resonator actuated electro-statically that showed shifts up to 4 ppm/V [30]. The smaller variation obtained with the lateral devices may be the result of the structure design, which features folded-beam anchors that may mitigate any changes in stress induced by the electrostatic force.

D. Electro-thermal mixing

Electro-thermal mixing has been performed on the cantilever and disk structures with Al u-shaped electrodes. Two input signals have been applied to the actuation electrodes (see Fig. 2b). Fig. 15 shows the resonant peaks measured when actuating electro-thermally a SiC cantilever and disk with two input signals. For the cantilever, when the two input signals have frequencies of f_1 = 50 kHz and f_2 = 39.91 kHz, the sum of the two results in a resonance peak at $f_1 + f_2$ = 89.91 kHz. The disk resonates at 892.65 kHz by setting f_1 = 400 kHz and sweeping f_2 from 450 kHz up to 550 kHz. The resonant peaks in Fig. 15 occur at the sum of the input frequencies. In addition, for a 50 µm long cantilever (f_0 = 945 kHz), by applying f_1 = 1200 kHz and f_2 = 255 kHz, a resonant peak has been detected at the difference of the two input frequencies $f_1 - f_2$ = 945 kHz [24].

From the comparison of the resonant peaks shown for electro-thermal actuation using one input (Fig. 7) and two inputs (Fig. 15), it can be seen that the mixing resonance is obtained approximately at the same value as the resonant frequency measured when applying one actuation signal. The structure performs a thermo-mechanical mix by converting the temperature fluctuations into mechanical vibrations. The resonant frequency that is measured when two input signals are applied has been found to be slightly higher than the value obtained when applying only one input signal (0.15% higher

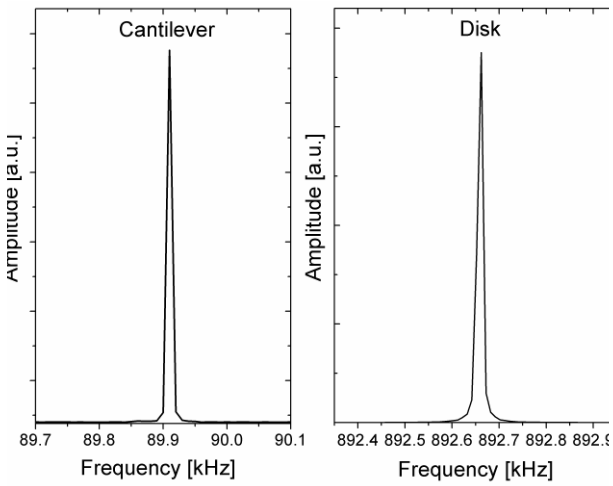

Fig. 15. Electro-thermal mixing: measured resonant peaks for cantilever (L = 200 µm) and disk (D = 380 µm).

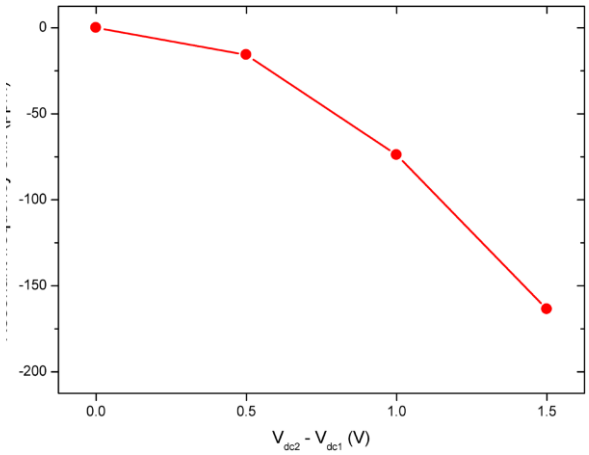

Fig.16. DC bias (V_{dc2} – V_{dc1}) variation: measured frequency shift relative to the value at 0 V DC bias for a disk resonator with u-shaped Al actuation electrode, while performing mixing.

for the disk and 0.55% higher for the cantilever). The difference is probably due to the lower DC voltage drop across the electrode in the mixing configuration.

E. Electro-thermal mixing and tuning

The effect of changing the DC bias of the two input signals applied to a disk resonator when performing mixing has been investigated. For this experiment, a disk resonator with u-shaped Al electrodes has been used. V_{dc2} has been held at 2 V while V_{dc1} has been varied from 2 V to 0.5 V. The AC voltages have been set at $V_{ac1} = V_{ac2} = 6$ V.

Fig. 16 shows the measured resonant frequency shift as a function of the increase of the DC voltage drop. The trend is the same as for bridges that have been actuated with one input signal. However, the overall value of the frequency shift for the disk resonator when operating in the mixing configuration (-110 ppm/V) is about 10 times less compared to a bridge with a slab electrode (-1,100 ppm/V) and 100 times less compared to a bridge with a u-shaped electrode (-11,000 ppm/V).

The smaller frequency shift measured for the disk can be explained by considering the larger area of the structure when compared to a bridge structure. In the case of disks, the electro-thermal heating is dissipated on a larger area compared to beam structures resulting in lower thermal expansion with respect to the initial structure size. Under these conditions, the compressive stress experienced by disk structures is expected to be lower compared to the one experienced by bridge ones, thus resulting in a smaller frequency shift.

V. Conclusions

SiC electro-thermal resonators have been designed, fabricated, simulated and tested. Cantilevers, bridges and disks with Al and Pt top electrodes have been studied. The fabricated devices have been shown to operate as electro-thermo-mechanical tunable resonators. In particular, the ability of performing electro-thermal filtering, tuning and mixing functions simultaneously with the bimaterial metal/SiC resonators has been investigated.

Cantilevers and bridges with length in the range 50 – 250 µm and disks with diameter in the range 90 – 300 µm have been fabricated. Mechanical and electro-thermal excitation techniques have been used to induce resonance to the fabricated devices. In agreement with the analytical equations, the measurements have confirmed that circular architectures resonate at higher frequencies compared to beam ones.

Electro-thermal actuation has been performed by applying an AC voltage (< 6 V) superimposed to a DC bias (< 2 V) across the top metal electrodes patterned with u-shaped and slab configurations. When compared to beam structures, disk resonators have shown superior performances in terms of achievable resonant frequencies (up to ~ 7 MHz) and Q-factors (up to ~ 23,000). The devices have been shown to operate both in vacuum and at atmospheric pressure. In particular, a disk with a diameter of 90 µm has shown vibration amplitudes of ~ 10 pm and ~ 5 pm at 7.79 MHz and 27.57 MHz for the first and second mode, respectively, at atmospheric pressure.

Tuning of the resonant frequency has been demonstrated electro-thermally on the Pt/SiC bridges by varying the DC bias and AC amplitude of the actuating voltage. Slab electrodes have been shown to induce frequency shifts of about -1,100 ppm/V and -800 ppm/V when increasing the DC and AC amplitudes, respectively. A larger tuning range has been achieved using u-shaped electrodes showing shifts of about -11,000 ppm/V and -1,800 ppm/V when varying the DC and AC amplitudes, respectively. Therefore, the u-shaped electrode configuration could be employed for implementing *coarse* DC and *fine* AC frequency tuning. FEM simulations have confirmed that as the actuating voltage increases, the compressive stress of the structures increases thus inducing a decrease in the resonant frequency. The frequency shift is maximised when tuning using u-shaped electrodes due to the higher temperature induced at the centre of the bridge thus enhancing the thermal expansion of the structure. Electro-thermal tuning has been investigated at different ambient

temperatures. Simulations and measurements have shown that as the temperature is risen from to 10˚C to 100 ˚C, the frequency shift increases together with the total compressive stress. The study of the influence of the ambient temperature on the frequency shift allows the prediction and adjustment of the devices' resonance in non-optimal operating conditions.

It is worth noting that the maximum frequency achievable when implementing electro-thermal tuning is the intrinsic resonance of the structure (i.e. the resonance when V_{dc} = 0 or V_{ac} = 0). Therefore, a SiC MEMS resonator should be designed to have a higher than desired intrinsic resonant frequency in order to enable electro-thermal tuning to be implemented.

The resonant frequency of our electro-thermal devices exhibit a greater sensitivity to DC and AC voltage variation than previous studies that have tuned the frequency of electro-statically actuated structures. Our results suggest that electro-thermal heating has a greater influence on resonator stress than an electro-static force.

Mixing of two input frequencies has been performed electro-thermally with SiC cantilevers and disks having u-shaped Al electrodes. Mechanical resonance has been detected when two actuating voltages have been applied with the sum or difference of their frequency matching the fundamental frequency of the structures. Electro-thermal tuning on a disk while performing frequency mixing has been achieved by varying the DC bias of one of the actuating voltages.

The results presented in this paper demonstrate the possibility of using SiC MEMS electro-thermal resonators for real time clock and frequency-setting applications. Electro-thermal *coarse* and *fine* tuning using u-shaped electrodes can be employed to set the resonance of a structure at a desired value and correct the frequency drifts caused by fabrication processes or operating conditions.

ACKNOWLEDGMENT

The authors would like to thank *Imec* for support and advice during the electro-thermal tuning experiments.

REFERENCES

[1] T. L. Cornelius, *MEMS/NEMS Handbook*, Springer, New York, 2006.

[2] K. C. Schwab and M. L. Roukes, "Putting Mechanics into Quantum Mechanics," *Physics Today*, 58, 7, p. 36, 2005.

[3] N. Tien, A. Ongkodjojo, R. Roberts and D. Li, "The future of MEMS in energy technologies," *Solid-State and Int.-Circ. Tech., ICSICT, 9th International Conference on*, 2452-2455, 2008.

[4] B. Tilmans, De Raedt, "MEMS for wireless communications: from RF-MEMS components to RF-MEMS-SiP," *J. of Micromech. and Microeng.*, 13, pp. S139-S163, 2003.

[5] C. Lam, "A review of the recent development of MEMS and crystal oscillators and their impacts on the frequency control products industry," *IEEE Int. Ultrasonics Symp. Proc.*, pp. 694-704, 2008.

[6] W.-T. Hsu, "Vibrating RF MEMS for Timing and Frequency References," *Microwave Symp. Dig., IEEE MTT-S Int.*, pp. 672-675, 2006.

[7] C. T.-C. Nguyen, "MEMS Technology for Timing and Freqeuncy Control," *IEEE Trans. on Ultrason., Ferroelec. and Freq. Cont.*, 54, pp.251-270, 2007.

[8] D. J. Young, I. E. Pehlivanoğlu and C. Zorman, "Silicon carbide MEMS-resonator-based oscillator," *J. of Micromech. and Microeng.*, 19, 110527, 2009.

[9] C. C.-T. Nguyen, "Vibrating RF MEMS for next generation wireless applications," *Custom Int. Circ. Conf., Proc. of the IEEE*, pp. 257-264, 2004.

[10] A. Wong, C. T.-C. Nguyen, "Micromechanical mixer-filters ("Mixlers")," *J. of MEMS*, 13, pp. 100-112, 2004.

[11] J. L. Skinner, P. M. Dentinger, F. W. Strong, S. E. Glanoulakis, "Low-power electrothermal actuation for microelectromechanical systems," *J. Micro/Nanolith. MEMS MOEMS*, 7(4), 043025, 2008.

[12] R. Reichenbach, M. Zalalutdinov, K. Aubin, R. Rand, B. Houston, J. Parpia, H. Craighead, "Third-order intermodulation in a micromechanical thermal mixer," *J. of MEMS*, 14, pp. 1244-1252, 2005.

[13] M. Mehregany, C.A. Zorman, N. Rajan and C.H. Wu, "Silicon Carbide MEMS for Harsh Environments," *Proc. IEEE*, 86, pp. 1594 – 1610, 1998.

[14] R. Cheung, ed., "*Silicon carbide microelectromechanical systems for harsh environments*", Imperial College Press, 2006.

[15] Y.T.Yang, K.L. Ekinci, X.M.H.Huang, L.M. Schiavone, M.L.Roukes, C.A. Zorman and M. Mehregany, "Monocrystalline silicon carbide nanoelectromechanical systems," *Appl. Phys. Lett.*, 78, pp. 162-164, 2001.

[16] T. Remtema, L. Lin, "Active frequency tuning for micro resonators by localized thermal stressing effects," *Sens. and Act. A*, 91, pp. 326-332, 2001.

[17] S.C. Jun, X.M.H. Huang, M. Manolidis, C.A. Zorman, M. Mehregany and J Hone, "Electrothermal tuning of Al-SiC nanomechanical resonators," *Nanotechnol., 17*, pp. 1506-1511, 2006.

[18] B. Sviličić, E. Mastropaolo, B. Flynn and R. Cheung, "Electrothermally actuated and piezoelectrically sensed silicon carbide tunable MEMS resonator," *IEEE Electron. Dev. Lett.*, 33, 278-280, 2012.

[19] E. Mastropaolo, R. Cheung, A. Henry and E. Janzen, "Electrothermal actuation studies of silicon carbide ring resonators," *J. Vac. Sci. Technol. B*, 27, pp. 3109-3114, 2009.

[20] T. Wakayama, T. Kobayashi, N. Iwata, N. Tanifuji, Y. Matsuda and S. Yamada, "Micro-fabrication of silicon/ceramic hybrid cantilever for atomic force microscope and sensor applications," *Sens. and Act. A*, 126, pp. 159-164, 2006.

[21] L. Jiang, R. Cheung, J. Hedley, M. Hassan, A.J. Harris, J.S. Burdess, M. Mehregany and C.A. Zorman, SiC cantilever resonators with electrothermal actuation, *Sens. and Act. A*, 128, pp. 376-386, 2006.

[22] P. Srinivasan and M. Spearing, "Effect of Heat Transfer on Materials Selection for Bimaterial Electrothermal Actuators," *J. of MEMS*, 17, pp. 653-667, 2008.

[23] V.L. Doughtie, A. Vallance and L.F. Kreisle, *Design of Machine Members*, McGraw-Hill, 1964.

[24] E. Mastropaolo, I. Gual and R. Cheung, "Silicon carbide electrothermal mixer-filters," *Elec. Lett.*, 46, pp. 62-63, 2010.

[25] C.A. Zorman, A.J. Fleischman, A.S. Dewa, M. Mehregany, C. Jacob, S. Nishino and P. Pirouz, "Epitaxial growth of 3C-SiC films on 4 in. diam (100) silicon wafers by atmospheric pressure chemical vapour deposition," *J. Appl. Phys.*, 78, pp. 5136-5138, 1995.

[26] E. Mastropaolo, I. Gual, G. Wood, A. Bunting and R. Cheung, "Piezo-electrically driven silicon carbide resonators", *J. Vac. Sci. and Technol. B*, 28, pp C6N18 - C6N23, 2010.

[27] N. O. V. Plank, M. A. Blauw, E. W. J. M. van der Drift, and R. Cheung, "The etching of silicon carbide in inductively coupled SF_6/O_2 plasma," *J. of Phy. D: App. Phys.*, 36, p. 482, 2003.

[28] G.S. Wood, I. Gual, P. Parmiter and R. Cheung, "Temperature stability of electro-thermally and piezoelectrically actuated silicon carbide MEMS resonators," *Microelec. Reliability*, 50, pp. 1977-1983, 2010.

[29] K. Babaei Gavan, H.J.R. Westra, E.W.J.M Van der Drift, W.J. Venstra and H.S.J. Van der Zant, "Impact of fabrication technology on flexural resonances of silicon nitride cantilevers," *Microelec. Eng.*, 86, pp. 1216-1218, 2009.

[30] W.-T. Chang and C. Zorman, "Electrical Characterization of Microelectromechanical Silicon Carbide Resonators," *Sensors*, 8, pp. 5759-5774, 2008.

[31] E. Mastropaolo, G.S. Wood and R. Cheung, "Electro-thermal behaviour of Al/SiC clamped-clamped beams," *Microelec. Eng.*, 87, pp. 573-575, 2010.

[32] S. Roy, R.G. DeAnna, C.A. Zorman and M. Mehregany, "Fabrication and Characterization of Polycrystalline SiC Resonators," *IEEE Trans. Electron. Dev.*, 49, pp. 2323-2332, 2002.

Enrico Mastropaolo received the *laurea* degree in microelectronics engineering from Univeristà degli Studi di Padova, Italy, in 2006, and the Ph.D degree in microsystems and microfabrication from The University of Edinburgh, U.K., in 2011.

He is currently working as a Research Fellow at the University of Edinburgh in the Scottish Microelectronics Centre. His research interests include design, simulations, fabrication and characterisation of MEMS devices, transduction techniques and SiC as structural material for MEMS devices.

Graham S. Wood (M'10) received the M.Eng degree in electronics and electrical engineering and the M.Sc by Research degree in microelectronics from the University of Edinburgh, U.K., in 2008 and 2011, respectively. He is currently working toward the Ph.D. degree in microelectronics at the University of Southampton, U.K.

From June 2008 until April 2010, he was a Research Associate with the Scottish Microelectronics Centre, University of Edinburgh, U.K., where he conducted research concerning the actuation and sensing of SiC MEMS resonators for high-frequency RF applications. His current research interests include the use of mode-localisation in electrically-coupled MEMS resonators for sensor applications.

Isaac Gual received the Bachelor's and Master's degree in telecommunication engineering from Universitat Politècnica de Catalunya (UPC), Catalonia, in 2004 and 2006, respectively. During this period he had internships with both Sony and Fraunhofer Institute.

After graduating, he worked as a Project Engineer from July 2006 to January 2007. He then joined the University of Edinburgh as a Research Associate in the Scottish Microelectronics Centre where his research focus was SiC MEMS resonators. Since 2010 he has been working as a Product Manager at Intesis Software, Barcelona.

Philippa Parmiter received the B.Eng (Hons) degree in electronic and electrical engineering and the Ph.D degree in physical electronics from Kings College London, U.K., in 1989 and 1993, respectively, and the M.Sc (Distinction) degree in environmental protection and management from the University of Edinburgh, U.K., in 2010, where she was awarded the Best Paper Award.

From 1993 to 1995, she was a Research Assistant in the physics dept. of Kings College London working on the fabrication of computer generated holograms for free-space optical communications. From 1995 to 2000, she was a Senior Semiconductor Process Technologist at DERA (now Qinetiq) where she worked on high power, high speed optical and microwave devices including wide bandgap FETs. In 2000, she worked on mixed-signal silicon design for an electronic nose at Glasgow University before starting at MicroEmissive Displays Ltd in January 2001, where she was involved in silicon backplane design and FPGA simulation before becoming Senior Applications Manager, managing her team and providing technical collateral to customers around the world. In 2009, she was with the University of Edinburgh and worked as a Research Manager in the Scottish Microelectronics Centre on a SiC MEMS resonators project funded by Scottish Enterprise as a proof of concept project. She currently works at the Scottish Institute of Sustainable Technology, Edinburgh.

Dr. Parmiter is a Chartered Engineer, MIET and holds a US patent *Travelling-wave guide electro-optic modulator*.

Rebecca Cheung (M'96–SM'02) received a first class honours and Ph.D degree in electronics and electrical engineering from the University of Glasgow, U.K., in 1986 and 1990, respectively. In 1986, she was awarded a Croucher Foundation scholarship to study towards a Ph.D. During her Ph.D, she was a visiting researcher at IBM Thomas J. Watson Research Centre, Yorktown Heights, USA, where high density plasma etching techniques were developed to form nanostructured GaAs.

From 1990 to 2000, she had been a visiting scientist with the Delft Institute of Microelectronics and Submicron Technology, The Netherlands; the Laboratory for Electromagnetic Fields and Microwave Electronics at ETHZ, Switzerland and the Nanoelectronics Research Center at the University of Glasgow, working on various topics related to semiconductor technology, process-induced materials damage, mesoscopic physics in SiGe heterostructures and microwave circuits in InP for gigabit electronics. Additionally, she had been a founding member of the "Nanostructure Engineering Science and Technology" (NEST) Group at the University of Canterbury, New Zealand in 1998. Currently, she holds a Chair in Nanoelectronics in the School of Engineering at the University of Edinburgh, U.K.

Prof. Cheung has an international reputation for her contribution in the development and application of micro- and nano- fabrication. More recently, her research focusses on micro-resonators and micro-electromechanical systems. She has published over 140 scientific articles with more than 85 peer-reviewed journal papers, including 15 invited review papers, 1 patent and 1 book. Professor Cheung serves in numerous scientific panels and committees, is a Fellow of the IET, and an Honorary Professor with the School of Engineering and Physical Sciences at Heriot-Watt University, U.K.